Genes Genom (2014) 36:387–397
DOI 10.1007/s13258-014-0186-9

RESEARCH ARTICLE

Functional analysis of the receptor binding domain of SARS coronavirus S1 region and its monoclonal antibody

Hyun Kim · Yeongjin Hong · Keigo Shibayama · Yasuhiko Suzuki · Nobutaka Wakamiya · Youn Uck Kim

Received: 30 September 2013 / Accepted: 31 March 2014 / Published online: 16 April 2014

Abstract Severe acute respiratory syndrome (SARS) is caused by the SARS coronavirus (CoV). The spike protein of SARS-CoV consists of S1 and S2 domains, which are responsible for virus binding and fusion, respectively. The receptor-binding domain (RBD) positioned in S1 can specifically bind to angiotensin-converting enzyme 2 (ACE2) on target cells, and ACE2 regulates the balance between vasoconstrictors and vasodilators within the heart and kidneys. Here, a recombinant fusion protein containing 193-amino acid RBD (residues 318–510) and glutathione S-transferase were prepared for binding to target cells. Additionally, monoclonal RBD antibodies were prepared to confirm RBD binding to target cells through ACE2. We first confirmed that ACE2 was expressed in various mouse cells such as heart, lungs, spleen, liver, intestine, and kidneys using a commercial ACE2 polyclonal antibody. We also confirmed that the mouse fibroblast (NIH3T3) and human embryonic kidney cell lines (HEK293) expressed ACE2. We finally demonstrated that recombinant RBD bound to ACE2 on these cells using a cellular enzyme-linked immunosorbent assay and immunoassay. These results can be applied for future research to treat ACE2-related diseases and SARS.

Keywords SARS coronavirus · Angiotensin-converting enzyme · Receptor binding domain · Monoclonal RBD antibody · Rennin–angiotensin system

H. Kim · K. Shibayama
Department of Bacteriology II, National Institute of Infectious Diseases, 4-7-1 Gakuen, Musashi-Murayama, Tokyo 208-0011, Japan

H. Kim · Y. U. Kim (✉)
Department of Biomedical Sciences, Sun Moon University, A-San 336-708, Republic of Korea
e-mail: kimyu@sunmoon.ac.kr

Y. Hong
Department of Microbiology and Clinical Vaccine R&D Center, Chonnam National University Medical School, Gwangju 501-746, Republic of Korea

Y. Suzuki
Division of Global Epidemiology, Hokkaido University Research Center for Zoonosis Control, Sapporo 001-0020, Japan

N. Wakamiya
Department of Microbiology and Immunochemistry, Asahikawa Medical College, Asahikawa, Japan

Introduction

Severe acute respiratory syndrome (SARS) is a fatal emerging infectious disease caused by the SARS coronavirus (CoV) (Baker 2004; Rota et al. 2003). SARS-CoV-like virus has been isolated from horseshoe bats in China, and this has been postulated to be the natural reservoir for the virus (Lau et al. 2005; Li et al. 2005b). Although there have been no recent SARS outbreaks, serious concerns remain about its re-emergence from host animals and its potential application as a bioterrorism agent (Chan et al. 2006; Peiris and Yuen 2004).

SARS-CoV mediates infection of target cells via the spike (S) protein, which is a type one transmembrane glycoprotein divided into two functional domains of S1 (15–680 a.a.) and S2 (681–1255 a.a.) (He et al. 2004a; Li et al. 2005a). Infection of SARS-CoV is initiated by binding of the S protein to the angiotensin-converting enzyme 2 (ACE2) functional receptor expressed on target cells (Li et al. 2003). A 193-amino acid fragment (residues 318–510) within the S1 subunit of the S protein has been characterized

as the minimal receptor-binding domain (RBD) (Wong et al. 2004). In early studies, mice immunized with inactivated SARS-CoV were used to generate monoclonal antibodies capable of blocking infectivity. Of these, several antibodies were directed against the S protein (Berry et al. 2004). The S protein serves as the main antigen that elicits protective immune responses, including neutralizing antibodies in infected humans and animals (Bisht et al. 2004; Buchholz et al. 2004; Greenough et al. 2005; Hofmann et al. 2004). Several studies have demonstrated that RBD of the S region is a major target for neutralizing SARS-CoV antibodies (He et al. 2004b, 2005; Zhou et al. 2004).

ACE2, also called ACEH (ACE homologue), is an integral membrane protein and a zinc metalloprotease of the ACE family that also includes somatic and germinal ACE (Komatsu et al. 2002; Tipnis et al. 2000). ACE2 has been implicated in the pathology of Hartnup's disease, a disorder of amino acid homeostasis, and it has been recently revealed that ACE2 controls intestinal inflammation and diarrhea via its function in amino acid transport; thus, regulating the gut microbiome (Kuba et al. 2013). Mouse ACE2 has about a 40 % amino acid identity to the N- and C-terminal domains of mouse somatic ACE. The predicted mouse ACE2 protein sequence consists of 798 amino acids, including an N-terminal signal peptide, a single catalytic domain, a C-terminal membrane anchor, and a short cytoplasmic tail. ACE2 is a newly described rennin–angiotensin (RAS) system component that is sensitive to chloride ion concentration (Donoghue et al. 2000). It is a membrane-bound enzyme that acts as a monocarboxypeptidase and is an essential regulator of heart function. Within the RAS, ACE2 competes with ACE because it is capable of hydrolyzing the inactive decapeptide angiotensin I (Ang I) into the nonapeptide Ang (1–9); thus, decreasing the amount of Ang I available for pressor Ang II generation by ACE. Similarly, ACE2 degrades the vasoconstrictor Ang II into vasodilator Ang (1–7), which may also be produced from Ang (1–9) hydrolysis by ACE (Donoghue et al. 2000; Vickers et al. 2002; Zhong et al. 2010). The antagonistic relationship between ACE and ACE2 modulates the balance between Ang II (vasopressor) and Ang 1–7 (vasodilator), which plays a significant role regulating renal and cardiovascular functions. SARS-CoV infections and the S protein decrease ACE2 expression, and S protein injections into mice worsen acute lung failure in vivo (Kuba et al. 2005). In contrast, ACE2 and the type 2 Ang II receptor protect mice from severe acute lung injury, but other components of the RAS (including ACE, Ang II, and Ang II type 1a receptor) promote disease occurrence (Imai et al. 2005). These findings suggest a possible therapeutic role for ACE2 in acute lung injury, which affects many people worldwide every year.

Expression of ACE2 is more restricted than ACE, which is widely distributed on the endothelial cells of the arteries, arterioles, and venules in the heart and kidneys (Tipnis et al. 2000; Oudit et al. 2003). ACE2 is also expressed in the vascular smooth muscle cells of the intrarenal arteries, the renal tubular epithelium, coronary blood vessels (Donoghue et al. 2000) and adult Leydig cells of the testis (Douglas et al. 2004). Other investigators have shown that ACE2 expression occurs on the surface of lung alveolar epithelial cells and enterocytes of the small intestine (Hamming et al. 2004). ACE2 mediates binding between a Vero E6–ACE2 expressing cell line and the recombinant S protein expressed on the surface of CHO cells, even under high stringency washing conditions (Chou et al. 2005).

ACE2 was recently reported at various levels in various tissues that also express ACE mRNA. Because ACE2 is a functional receptor for the SARS-CoV, its tissue distribution seems to be of great importance and appears to be species specific. ACE2 may also contribute to programmed hypertension.

Here, we report that a recombinant RBD fusion protein induced a high titer of RBD-specific monoclonal antibodies, and effectively operated the antigen protein. Our cellular enzyme-linked immunosorbent assay (ELISA) and competitive binding assay using a polyclonal ACE2 antibody indicated that our prepared recombinant RBD fusion protein binds to various tissues as well as NIH3T3 and HEK293 cells through ACE2. We think that our prepared recombinant RBD and its monoclonal antibody can be developed to prevent SARS and disease pathogenesis.

Materials and methods

Reagents and cells

The pGEX-4T-1 plasmid was purchased from GE (GE Healthcare Life Sciences, Uppsala, Sweden) to express the RBD-GST fusion protein. Goat anti-mouse IgG alkaline phosphatase and 4-nitrophenyl phosphate (NPP) were provided by Sigma (St. Louis MO, USA) for the ELISA. Dulbecco's modified Eagle's medium (DMEM) was purchased from Gibco (Grand Island, NY, USA) for hybridoma cell culture, and HAT and HT were obtained from Sigma for selecting the hybridoma cells. SP2/0 myeloma, HEK293, and NIH3T3 cells were provided by the American Type Culture Collection (Rockville, MD, USA) for preparing the hybridoma cell and cellular ELISA, respectively. Various tissues were lysed from Balb/c mice purchased from SLC (Tokyo, Japan) for detecting ACE2 expression. Alexa Fluor 488 reactive dye was purchased from Invitrogen (Carlsbad, CA, USA) to obtain confocal

images. All other chemicals used were of the best grade available from commercial sources.

Construction and expression of the RBD fusion protein

The PCR fragments encoding 193-a.a RBD sequences were amplified was done with two primers, SRAR6 (5′-GTCCG CGAATTCAACATCACCAACCTGTG) and SARS7 (5′-CTTCGGCTCGAGCACGGTGGCGGGCGCGT) against codon-optimized SARS spike protein gene in pcDNA3.1 (a gift of Dr. M. Farzan, Harvard Medical School, MA) as template in polymerase chain reaction (PCR). The PCR fragments were digested with *Eco*RI and *Xho*I and ligated into the same sites of the pGEX 4T-1 vector (GE Healthcare Bio-Sciences Corp, NJ, USA). As result, the expression plasmid carries an N-terminal glutathione-S-transferase (GST)-Tag/thrombin/*lac* promoter. The nucleotide sequence analysis was performed using the Dye Terminator Cycle Sequencing Ready Reaction kit with an ABI 373 DNA Sequencer.

The recombinant plasmid was transformed into competent *E. coli* BL 21 codon plus, and grown with constant shaking in 2× YT broth (20 g tryptone, 10 g yeast extract, 10 g NaCl/L) in the presence of ampicillin (50 μg/ml). Five ml of cell suspension was inoculated into 50 ml 2× YT fresh media/250 ml flask for induction of the recombinant protein and was incubated at 37 °C until optical density reached 0.6. The culture suspensions were further incubated for 4 h at 37 °C in the presence of 0.5 mM isopropyl-β-D-thio-galactoside with vigorous shaking (180 rpm). Four ml of bacterial culture was harvested by centrifugation at 4 °C, and the pellet was resuspended with 4 ml of reduced sodium dodecyl sulfate polyacrylamide gel electrophoresis (SDS-PAGE) sample buffer. The reactions were heated at 95 °C for 5 min, and only the supernatant was applied to 13 % SDS-PAGE gels using a mini-protein electrophoresis apparatus (Bio-Rad Hercules, CA, USA). The gel was soaked in 0.2 M cold KCl solution for 10 min until the protein bands appeared as a gray color, then the bands were cut with a razor for homogenizing. The chopped gel and 0.5 ml PBS were added to a microtube for homogenizing, and about 30 strokes were done to crush the gel. The tube was centrifuged for 30 min at 15,000×*g* to remove the gel piece and then filtered with a 0.2 μm filter. Purity was confirmed by 13 % SDS-PAGE and used to immunize mice to prepare a monoclonal antibody.

Preparation of the RBD monoclonal antibody

The purified RBD fusion protein was mixed with an equal volume of complete Freund's adjuvant (Sigma) and injected intraperitoneally. The antigen-adjuvant mixture was injected into female Balb/c mice (8 weeks old). The first injection was followed by three booster injections at 3- or 4-week intervals. The final injection was administered without adjuvant 3–4 days before cell fusion. After confirming the antibody titer in tail blood from immunized mice, B cells were separated from the spleen for fusion with myeloma cells. Feeder cells were prepared 1 day before fusion from a 15 week-old mouse. The abdominal skin was carefully removed and feeder cells were collected by centrifugation. The fusion experiments were performed as follows. Spleen cells were released by tearing the removed spleen with forceps and the rough side of a slide glass, and the cells were collected in a 15 ml centrifuge tube. The spleen cells and Sp2/0-Ag-14 mouse myeloma cells were mixed in a 10:1 ratio, and 1 ml of 50 % polyethylene glycol 4000 in serum-free DMEM was added slowly. The fusion process was allowed to continue for 1 min at 37 °C and centrifuged for 2 min at 100×*g*. Then, 4.5 ml DMEM was added slowly for the first 3 min, and 5 ml was added over the next 2 min. The fused cells were brought up to 50 ml with DMEM, and collected by centrifugation at 100×*g* for 5 min. The cells were carefully resuspended in 35 ml of selective HAT medium [DME supplemented with 20 % fetal bovine serum (FBS), antibiotics, and HAT] by swirling, and then incubated under 8 % CO_2 for 30 min. Each 100 μl of cell suspension was transferred to 96-well plates, and incubated under 8 % CO_2 in an incubator. About 2 weeks after the fusion, culture supernatants were collected and screened by ELISA. Positive clones were transferred to 6-well plates, and frozen in liquid nitrogen. All positive clones were frozen first and cloned by limiting dilution after thawing.

Purification of the monoclonal antibody

Hybridoma cells (1×10^7) were intraperitoneally injected into a Balb/c mouse to collect ascites and purify the monoclonal antibody. After 2 weeks, the drained ascites were centrifuged for 30 min at 15,000×*g* to remove residual cells and insoluble aggregates and then applied to a Protein G-agarose column (HiTrap 5 ml, GE Healthcare Life Sciences). The column was washed with phosphate-buffered saline (PBS) until the absorbance of unbound proteins decreased to background, and then the antibody was eluted with 0.1 M glycine–HCl, pH 2.5. The eluted antibody was neutralized by adding 1 M Tris and dialyzed against PBS overnight.

ELISA

A 96-well micro titer plate (Costar, Boston, MA, USA) was coated with 50 μl (5 μg/ml) of purified RBD fusion and GST proteins at 4 °C overnight and then was washed three times with deionized distilled water. The wells were blocked with 250 μl blocking buffer (borate buffered saline

containing 5 % skim milk, 1 mM EDTA, 0.05 % NaN_3, and 0.05 % Tween 20) for 30 min at room temperature. After three washes with blocking buffer, 50 µl of antiserum or cell supernatant was added and incubated for 2 h at room temperature. The wells were washed three times with water, and then blocked with blocking buffer for 30 min at room temperature. A goat anti-mouse IgG antibody coupled with alkaline phosphatase (Sigma, 100 µg/ml in blocking buffer) was incubated at room temperature for 2 h to bind the first antibody.

The 96-well plates were washed with water and detected with 100 µl of 1 mg/ml (3 mM) p-NPP in 0.05 M Na_2CO_3 and 0.05 mM $MgCl_2$. The reaction was stopped with 25 µl of 0.5 M NaOH and measured at 405 nm using a microtiter plate reader (Bio-Rad).

For the cellular ELISA, various tissues were separated from the Balb/c mouse and treated with ammonium sulfate to remove the erythrocytes. The cells were washed and cultured with 10 % FBS/DMEM media, then transferred to a 96-well plate at 5×10^5 cells/well for immobilizing cells to the plate. The wells were washed with PBS, and 150 µl of 1 % paraformaldehyde was added (ethanol:methanol = 1:1). The plate was incubated for 30 min at −20 °C and washed with water to react the RBD or ACE2 antibody (Rabbit IgG polyclonal antibody, Cat # 18-661-15167, GenWay Biotech, CA, USA). Paraformaldehyde fixation has been used to attach various primary tissue cells and established cell lines to plastic wear or slide glass. We used paraformaldehyde fixation because we worried about detachment of primary tissue cells and suspension cells from vessel during various experimental procedures. For example, in our cellular ELISA, intact cell was attached to plastic wear in the first step, and then several reactions such as RBD or Ab were successively followed.

Western blot analysis

The RBD fusion protein or tissue cell lysates were suspended in reduced SDS-PAGE sample buffer and heated, then resolved on 12 % SDS-PAGE. The gels were electrophoretically transferred to PVDF membranes using a mini protein II transfer chamber (Bio-Rad). The membranes were blocked overnight at 4 °C in PBS containing 5 % skim milk, and then washed three times with PBS containing 0.1 % Tween 20 (PBS-T). Sequentially, the membrane was washed two times with PBS-T and incubated with 5 µg/ml RBD or ACE2 antibody for 1 h. After washing twice with PBS-T, the membrane was reacted with goat anti-mouse IgG antibody coupled with alkaline phosphatase for 2 h at room temperature. The membranes were washed five times with PBS-T and five times with distilled water, then developed using 1 mg/ml (3 mM) (NPP in 0.05 M Na_2CO_3, 0.05 mM $MgCl_2$.

Immunofluorescence assay

NIH3T3 and HEK293 cells were cultured and transferred to a four-chambered flask for fluorescence labeling and imaging. After washing with PBS, paraformaldehyde solution (4 %) was added to the cells and incubated for 30 min at 4 °C to fix the cells to the wells. After three washes with PBS, 0.2 % Triton X-100 was added to the plate for 30 min at 4 °C. The plate was washed three times with PBS, and then 1 % BSA (in PBS) was added and incubated for 1 h at room temperature. After washing with PBS, the RBD fusion protein was incubated for 1 h at room temperature to bind with the ACE2 molecules on the cell membranes. After washing three times with PBS, the monoclonal RBD antibody was reacted with the RBD-ACE2 binding reactant. Finally, secondary antibody (goat anti-mouse IgG coupled with Alexa 488-green) was treated for 1 h at room temperature and sequentially with DAPI for 30 s. Cell imaging was performed using an Olympus FV1000 confocal microscope equipped with a four-laser system (Multi AR laser, HeNe G laser, HeNe R laser, and LD405/440 laser diode) with transmitted light, differential interference contrast, and complete integrated image analysis software system (Olympus America Inc., Melville, NY, USA). The excitation and emission wavelengths for Alexa Fluor 488 (green) and DAPI (red) were 488/520 and 543/570 nm, respectively. Composite digital images were then converted to TIFF format, imported into Adobe Photoshop (Adobe Photoshop CS2, version 9.0; Adobe Systems Inc., San Jose, CA, USA), and color balance was adjusted for presentation.

Results

Expression and purification of the RBD-GST fusion protein and preparation of the monoclonal RBD antibody

PCR products of 579 bp (193 a.a.) long RBD sequences were ligated to the pGEX 4T-1 expression vector and expressed in *E. coli* BL 21 (Fig. 1a). Main bands of 48–50 kDa (Fig. 1a, lane 1) and 25 kDa (Fig. 1a, lane 2) were detected in *E. coli* extracts, which transformed RBD-GST and GST DNA, respectively. As shown Fig. 1b, the two main bands were purified for immunization into five mice each. After the final injection of purified antigen, the antibody titer was checked in tail blood. After 3–4 days, mouse spleen cells were lysed and fused with myeloma cells to prepare hybridoma cells. After limiting dilutions for 4 weeks, we obtained seven RBD fusion and five GST positive colonies, respectively. Among the seven positive colonies against the RBD-GST fusion protein, four colonies reacted only with the RBD but not the GST protein. The two colonies in the best condition were

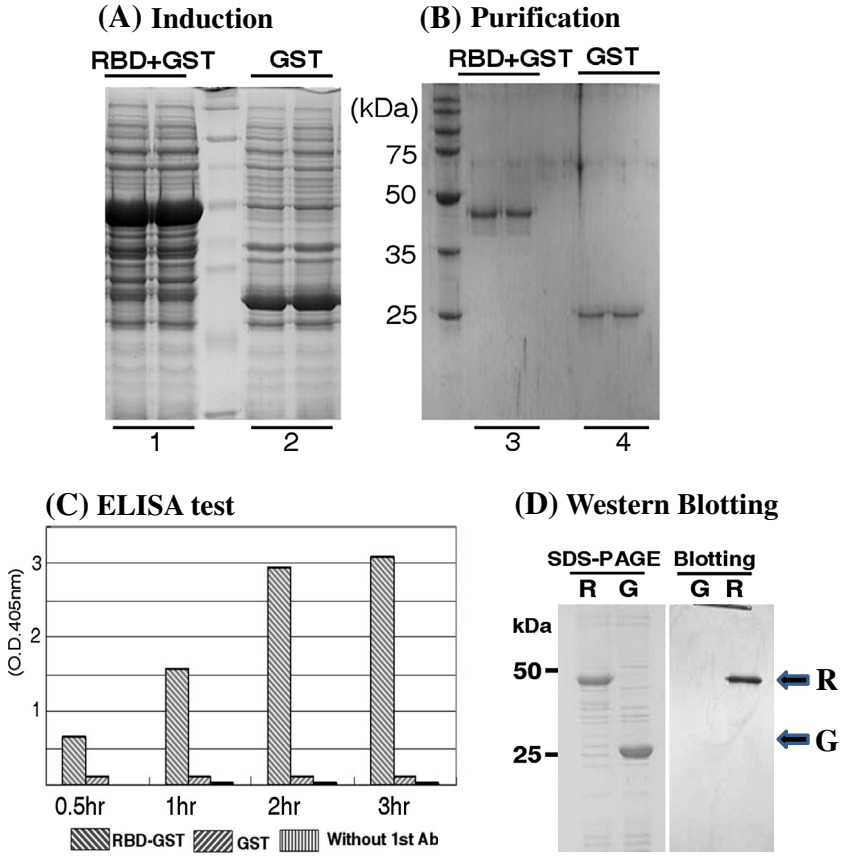

Fig. 1 Expression of the receptor-binding domain (RBD)+glutathione-S-transferase (GST) fusion and GST protein. **a** Induced *E. coli* total protein of RBD fusion and GST was applied to 13 % sodium dodecyl sulfate polyacrylamide gel electrophoresis (SDS-PAGE) and stained with Coomassie Brilliant Blue. **b** Purified protein from SDS-PAGE gel by gel lysing methods. Each gel shows the protein marker on the *left side*. **c** After a limiting dilution of the positive colony, the cell supernatants were analyzed by enzyme-linked immunosorbent assay. The GST protein was used as a negative control. After reacting the RBD-GST or GST protein and hybridoma supernatant, AP-conjugated goat anti-mouse and NPP substrate were reacted for reading at 405 nm in a DYNEX spectrophotometer. **d** The fusion and GST protein (1 μg/μl) were loaded on to a 13 % SDS-PAGE gel for immunoblot analysis. The *arrowed markers* 50 and 25 indicate the RBD+GST fusion protein and GST protein, respectively. Antibody was visualized with alkaline phosphatase-conjugated goat anti-mouse IgG. (*R* RBD+GST fusion protein; *G* GST protein)

expanded for intraperitoneal injection to obtain a large amount of antibody. The antibodies were purified from ascites, and assayed by ELISA and Western blotting as shown Fig. 1c, d. The results indicated that the selected monoclonal antibody recognized the RBD but not the GST region of the RBD-GST fusion protein (Fig. 1d).

Confirmation of RBD fusion protein binding to mouse tissues

Cells were separated from the heart, spleen, and liver to confirm binding to the cell surface. These cells were fixed to 96-well plates with paraformaldehyde, and treated using the same procedure as for the general ELISA. As shown Fig. 2a, three kinds of cells (heart, spleen, and liver) reacted to the RBD surface molecule. This binding phenomenon was confirmed by Western blotting analysis with the same cell lysates (Fig. 2b). The RBD fusion protein band appeared at ~50 kDa but not the GST protein in all three panels for the positive and negative controls. These three blotted membranes were successively treated with purified RBD fusion protein and RBD monoclonal antibody. Tissue cell lysates of heart or spleen revealed proteins at ~60 kDa. But, liver cells showed a smeared, faint band (Fig. 2b). This experiment indicated that our prepared RBD fusion protein bound to molecule(s) on the tissue cell surface.

Determining the RBD binding molecule for various mouse cells

Various cells were prepared from a Balb/c mouse, and the total cell lysates were loaded onto a 13 % gel for Western blotting analysis (Fig. 3). Similar to Fig. 2b, about a 60 kDa band was shown in various cell extracts (Fig. 3a). Among the various cells, heart and lung extracts showed strong bands that were two or three fold more intense than

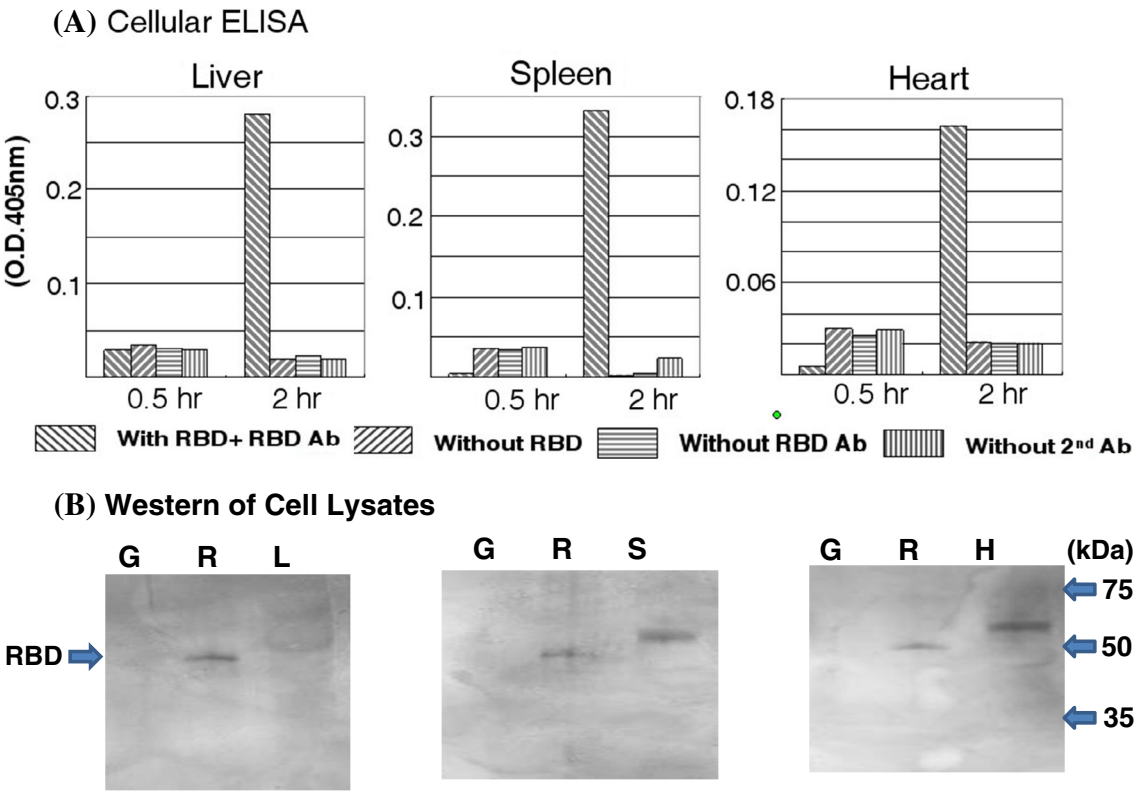

Fig. 2 Cellular enzyme-linked immunosorbent assay and Western blot analysis of mouse tissues. **a** Various mouse tissues were cultured and then fixed with paraformaldehyde. After reacting with receptor-binding domain (RBD)-specific monoclonal antibodies, alkaline phosphatase-conjugated goat anti-mouse IgG and NPP substrate were successively added to each well and measured in a DYNEX spectrophotometer at 405 nm. **b** To confirm the RBD receptor, whole cell lysates from mouse organ tissue cells were loaded on to 13 % sodium dodecyl sulfate polyacrylamide gel electrophoresis and immuno-blotted using the RBD monoclonal antibody. *Each lane* indicated as follows: *S* spleen; *L* liver; *H* heart; *G* glutathione-S-transferase (GST); *R*, RBD-GST

those of other extracts under the same cell preparation, indicating that the two kinds of cells may have been expressing the RBD binding protein.

Some studies have reported that the SARS virus is related to ACE. Thus, we tested ACE and ACE2 molecules as RBD receptors, and their antibodies were used as a blocking agent for RBD binding. As shown Fig. 3b, the ACE2 antibody was pretreated for 30 min before the RBD reaction to block the RBD receptor, and the RBD antibody was added to detect residual RBD binding (Fig. 3b). The 60 kDa band almost disappeared in the tissue cell lanes, but not from the RBD protein lane. We knew that this 60 kDa band corresponded to the ACE2 molecule that was detected at about the 60 kDa position with an ACE2 antibody (Fig. 3c). These results indicate that RBD bound to the ACE2 molecule in various cells.

Confirmation of RBD binding in established HEK293 and NIH3T3 cell lines

To confirm whether the RBD would bind to established cell lines, HEK293 and NIH3T3 cells were fixed in 96-well plates as shown in Fig. 2a. The cells were successively treated with RBD and RBD antibody. As shown Fig. 4a, the RBD protein bound to both cell types to the same extent. The same amounts of RBD protein and ACE2 antibody were simultaneously incubated with the cells for 30 min and detected with the RBD antibody (Fig. 4b; column 3). In this competitive assay, the ACE2 antibody suppressed 60–70 % of RBD binding in both cell lines within 30 min. We showed that these cell lines express ACE2 molecule 1 and that the molecules were the RBD receptor molecules as shown in the various mouse tissues. But, in this reaction, inhibition decreased 20–30 % after 3–4 h incubation (data not shown). It seemed that the ACE2 antibody may easily separate from the ACE2 molecule or was degraded.

Next, we examined whether RBD binding was blocked by the ACE2 antibody in a Western blot using mouse tissue cell lysates with a pair of membranes. The ACE2 molecule appeared as three or more bands in HEK293 cells and as two bands in NIH3T3 cell lysates (Fig. 4c, left panel). The other transferred membrane was pretreated with ACE2 antibody before RBD and RBD antibody to block the RBD

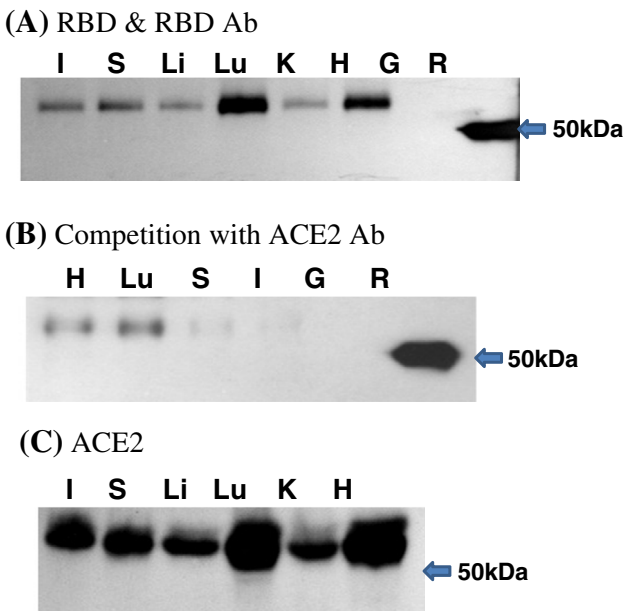

Fig. 3 Competition assay of receptor-binding domain (RBD) binding using the angiotensin-converting enzyme 2 (ACE2) antibody. **a** Various tissues lysates were loaded on to 13 % gels for sodium dodecyl sulfate polyacrylamide gel electrophoresis. Then, RBD and the RBD antibody were successively incubated to detect the RBD binding receptor. **b** Prior to adding the RBD fusion protein to the blotted membrane, the antiACE2 polyclonal antibody was reacted to block RBD binding. **c** Tissues cell lysates were reacted with ACE2 polyclonal antibody to confirm the presence of ACE2 molecules. *Each lane* is indicated as follows: *I* intestine; *S* spleen; *Li* liver; *Lu* lung; *K* kidney; *H* heart; *G* glutathione-S-transferase (GST); *R* RBD-GST

binding sites (Fig. 4c, right panel). Expectedly, ACE2 molecules in HEK293 cells were blocked with the ACE2 antibody but not in NIH3T3 cells. We confirmed this by confocal immunofluorescence image using the two cell lines that were fixed and treated with RBD and the RBD antibody (Fig. 5). As a result, the RBD receptor (ACE2) was observed in both HEK293 and NIH3T3 cells using the RBD antibody. A cocaine monoclonal antibody was used as the negative control in this experiment.

In this study, the reason why we used ELISA or immunoflourescence instead of immunoprecipitation or frozen section staining is that we want to investigate NIH3T3 or HEK293 cell lines and primary tissues cell at same condition and environment.

Discussion

The S protein of SARS-CoV is able to induce protective antibodies from infected animals (Bisht et al. 2004; Buchholz et al. 2004). The RBD (residues 318–510) in the S1 region of the S protein induces highly potent neutralizing antibodies against the SARS-CoV (He et al. 2004a, b). Here, we expressed the RBD of the S protein and immunized a mouse to prepare monoclonal antibodies. The RBD protein was prepared with the GST fused form and purified fusion protein without separating the two kinds of proteins, because this fusion protein was efficiently expressed in this system and easily separated from a gel. Another benefit is that the fused protein efficiently provided monoclonal antibodies due to its suitable molecular size (see Fig. 1). We also prepared a plural GST antibody for confirming the RBD specific binding experiments (data not shown). We have demonstrated with a cellular ELISA assay that RBD bound to cell membranes and that the anti-RBD antibody worked well with its antigen.

The first essential step of CoV infection is interaction of the S protein via the RBD with a specific cellular receptor. There are many reports that RBD plays a role infecting host cells. The RBDs on the S proteins of other CoVs such as mouse hepatitis virus, transmissible gastroenteritis virus, and human coronavirus also contain major antigenic determinants capable of binding to host cells (Bonavia et al. 2003; Godet et al. 1994). Some studies have reported that RBD-specific antibodies block receptor binding and virus entry (He et al. 2004a). Therefore, the RBD of the S protein may serve as an important target site for developing SARS vaccines and immunotherapeutics.

In this study, we conducted two kinds of experiments to demonstrate the results of previous reports. The first was cellular binding of RBD using a cellular ELISA as an intact cell instead of a traditional protein or antigen, and the second was Western blot analysis using the same cell lysates as in the cellular ELISA. In the cellular ELISA data, we demonstrated that the binding was due to RBD not GST, because the RBD fusion protein included the GST protein. This was shown by using the anti-GST antibody (data not shown), and the RBD binding receptor clearly appeared as a 60 kDa protein in the spleen and heart but was smeared in the liver lysate (Fig. 2b). The smeared band in the liver may indicate degradation by proteolysis or something that occurred during extract preparation, because this band was shown in other preparations (Fig. 3a).

There are many reports of SARS S or RBD protein binding to ACE2 on host cell membrane proteins using an antibody against SARS-CoV and by other methods. Various neutralizing monoclonal antibodies against SARS-CoV recognize overlapping sets of residues relative to the ACE2 molecule (Zhu et al. 2007). ACE2 is predominantly expressed in the heart, kidneys, and testes and at lower levels in a wide variety of tissues, particularly the colon and lungs (Lew et al. 2008). It seems that this RBD region plays a critical role attaching the host ACE2 molecule. This phenomenon was also supported by chimeric monoclonal antibodies that bind to the ACE2 RBD of the SARS S

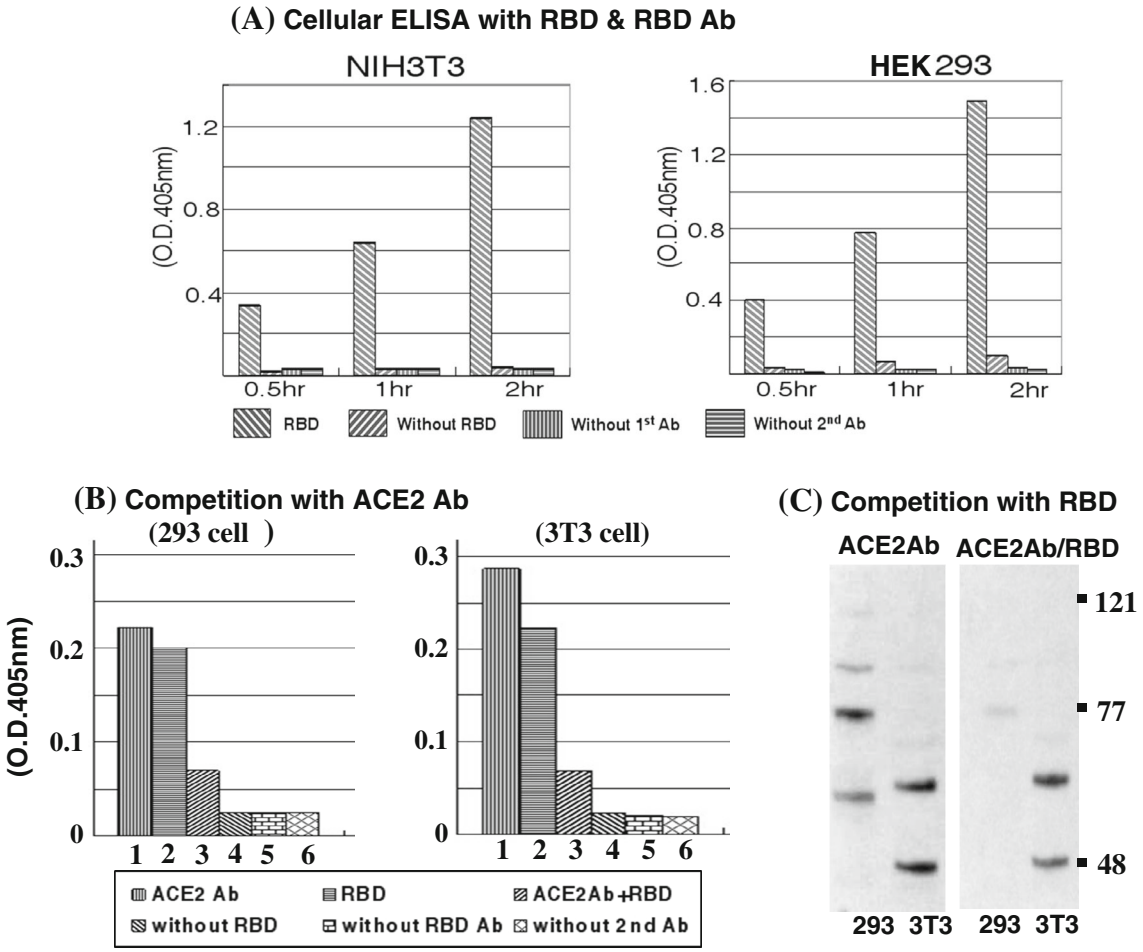

Fig. 4 Cellular enzyme-linked immunosorbent assay (ELISA) of established cell lines. **a** Each *cell line* was cultured and then fixed with paraformaldehyde. After reacting with the receptor binding domain (RBD) and RBD monoclonal antibody, alkaline phosphatase-conjugated goat anti-mouse IgG was added to each well. The *Plates* were developed with NPP substrate solution, and then read at 405 nm in a DYNEX spectrophotometer. **b**, **c** Competition assay by cellular ELISA (**b**) and Western blot (**c**). Prior to treatment with the RBD protein, the angiotensin-converting enzyme 2 (ACE2) polyclonal antibody was treated for 30 min to block the RBD binding site. Then, the RBD-specific monoclonal antibody and each secondary antibody were sequentially added to the cells

protein (Berry et al. 2010). Experimental support for ACE2-RBD binding was provided from a study of SARS antibody fragments competing with ACE2 for binding to the RBD (Prabakaran et al. 2006; Sui et al. 2004; Hwang et al. 2006). The crystal structure of the RBD–ACE2 complex has been identified, providing detailed information concerning RBD structure and function (Li et al. 2005a). The structure revealed that the RBD can be further divided into two separate subdomains. One is the RBD core and the other is the RBD loop (RPM) (a.a. 424–494). The RBD loop is the region that directly contacts the ACE2 molecule. In contrast, the RBD core contacts accessory proteins (Li et al. 2005a). We showed competitive binding of the RBD with the anti-ACE2 antibody (see Figs. 3, 4, 5). The same weights of tissue were homogenized and lysed by reducing SDS-PAGE sample buffer for Western blotting analysis. ACE2 was detected by the anti-ACE2 antibody in all of our organ tissue samples, which cross-reacts with the mouse/human ACE2 molecule.

ACE2 contains seven potential *N* linked glycosylation sites and is therefore likely to be glycosylated. Overexpressed ACE2 migrates at 120 kDa compared with the deglycosylated polypeptide that migrates at 85 kDa (Lew et al. 2008). Very low levels of ACE2 were detected in plasma by Western blot analysis and in multiples smaller than the full-length enzyme. This likely resulted from proteolytic cleavage (Lew et al. 2008). An approximately 90-kDa immunoreactive band was present in the whole-cell lysate, and a slightly smaller band was detected in the conditioned medium of ACE2-transfected cells, indicating that full-length ACE2 is processed in CHO cells to generate a secreted form (Donoghue et al. 2000).

We report, for the first time, that our prepared recombinant RBD bound to various mouse tissues and established

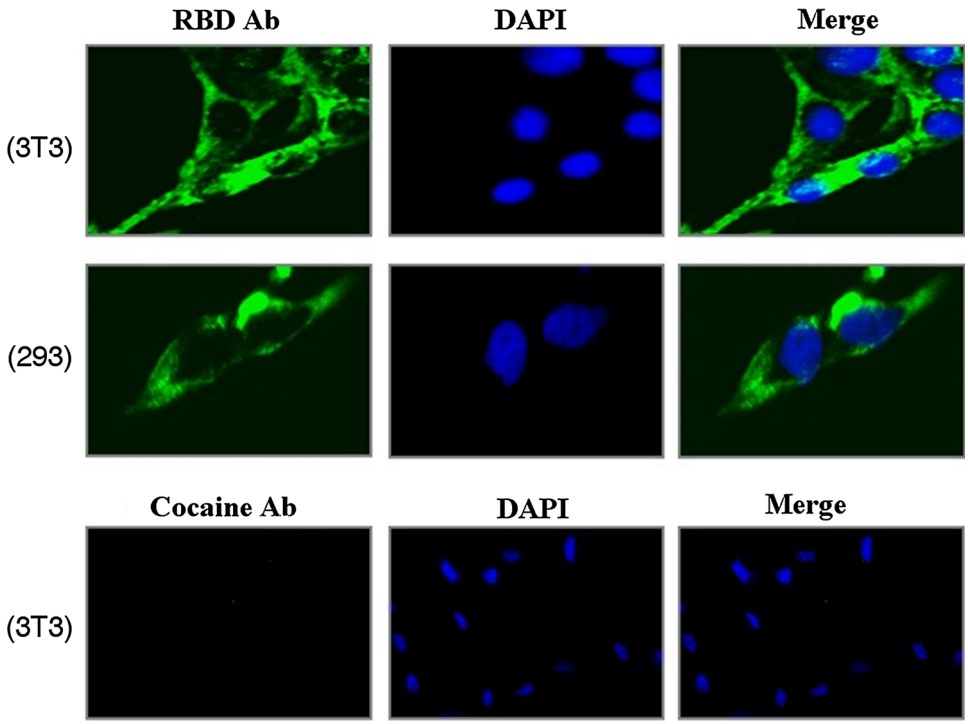

Fig. 5 Confocal microscope of established cell lines. NIH3T3 and HEK293 cells were reacted with the receptor binding domain (RBD) protein, and then the RBD monoclonal antibody and secondary Alexa 488 antibody were sequentially added to the each cell line, respectively. An anti-cocaine monoclonal antibody was used for the negative control. Green color indicates RBD binding to the cell surface. Nucleus was specifically stained by DAPI (*blue color*)

cell lines. The ACE2 molecule was detected at approximately 60 kDa and expressed strongly in the heart and lungs of mice. This is different from humans in which there is stronger expression in the kidneys than that in the lungs. RBD binding to ACE2 molecule was interfered with by pre-treatment with the ACE2 antibody in mouse tissues (see Fig. 3). We confirmed these results in NIH3T3 and HEK293 cells by cellular ELISA and a competitive assay (see Fig. 4a, b). The anti-ACE2 antibody suppressed RBD-ACE2 binding about 70–80 % within 30 min, but the inhibition decreased to 30–50 % after a 2–3 h incubation (data not shown). It seemed that the ACE2 antibody separated from the ACE2 molecules after a long incubation or degraded during incubation. We confirmed the molecular weight of ACE2 in HEK293 and NIH3T3 cells for the competitive assay in gels. Expressed ACE2 was 120 kDa, but it differs in tissue and cell lysates (Donoghue et al. 2000; Lew et al. 2008). In our lysates, ACE2 molecules occurred in three or more bands in HEK 293 cells and in two or more bands in NIH3T3 cells. This seemed to be a proteolytic cleavage pattern resulting from the different tissue lysate preparations (see Fig. 4c, left panel). The ACE2 molecules were completely blocked by the ACE2 antibody before treatment with the RBD protein in HEK293 cells, but not in NIH3T3 cells (see Fig. 4c, right panel). We suggest that the RBD binding site on ACE2 molecules in NIH3T3 cells may have been destroyed or changed due to cleavage of the ACE2 molecules during sample preparation. This suggestion was supported by our confocal microscope images results in which NIH3T3 cells stained well with the RBD fusion protein as in the HEK293 cells.

Here, we first confirmed that ACE2 was expressed in various mouse cells such as heart, lungs, spleen, liver, intestine, and kidneys using a commercial ACE2 polyclonal antibody. We also confirmed that the mouse fibroblast (NIH3T3) and human embryonic kidney cell lines (HEK 293) expressed ACE2. We finally demonstrated that recombinant RBD bound to ACE2 on these cells. We also demonstrated that our preparing RBD elicited high antibody titers in its immunized mice. Therefore, it appears to be an ideal immunizing antigen for generating monoclonal antibodies as well as a possible vaccine candidate. We have also found that the RBD binds to various tissues through ACE2. These results can be applied for future research to help treat ACE2 related diseases and SARS.

Acknowledgments This work was supported by the Sun Moon University Research Grant of 2010.

Conflict of interest The authors declare no conflict of interest.

References

Baker SC (2004) Coronaviruses from common colds to severe acute respiratory syndrome. Pediatr Infect Dis J 23:1049–1050

Berry JD, Jones S, Drebot MA, Andonov A, Sabara M, Yuan XY, Weingartl H, Fernando L, Marszal P, Gren J (2004) Development

and characterisation of neutralising monoclonal antibody to the SARS-coronavirus. J Virol Methods 120:87–96

Berry JD, Hay K, Rini JM, Yu M, Wang L, Plummer FA, Corbett CR, Andonov A (2010) Neutralizing epitopes of the SARS-CoV S-protein cluster independent of repertoire, antigen structure or mAb technology. mAb 2:53–66

Bisht H, Roberts A, Vogel L, Bukreyev A, Collins PL, Murphy BR, Subbarao K, Moss B (2004) Severe acute respiratory syndrome coronavirus spike protein expressed by attenuated vaccinia virus protectively immunizes mice. Proc Natl Acad Sci USA 101:6641–6646

Bonavia A, Zelus BD, Wentworth DE, Talbot PJ, Holmes KV (2003) Identification of a receptor-binding domain of the spike glycoprotein of human coronavirus HCoV-229E. J Virol 77:2530–2538

Buchholz UJ, Bukreyev A, Yang L, Lamirande EW, Murphy BR, Subbarao K, Collins PL (2004) Contributions of the structural proteins of severe acute respiratory syndrome to protective immunity. Proc Natl Acad Sci USA 101:9804–9809

Chan PKS, Tang JW, Hui DSC (2006) SARS: clinical presentation, transmission, pathogenesis and treatment options. Clin Sci 110:193–204

Chou CF, Shen S, Tan YJ, Fielding BC, Tan TH, Fu J, Xu Q, Lim SG, Hong W (2005) A novel cell-based binding assay system reconstituting interaction between SARS-CoV S protein and its cellular receptor. J Virol Methods 123:41–48

Donoghue M, Hsieh F, Baronas E, Godbout K, Gosselin M, Stagliano N, Donovan M, Woolf B, Robison K, Jeyaseelan R (2000) A novel angiotensin-converting enzyme-related carboxypeptidase (ACE2) converts angiotensin I to angiotensin 1–9. Circ Res 87:E1–E9

Douglas GC, O'Bryan MK, Hedger MP, Lee DK, Yarski MA, Smith AI, Lew RA (2004) The novel angiotensin-converting enzyme (ACE) homolog, ACE2, is selectively expressed by adult Leydig cells of the testis. Endocrinology 145:4703–4711

Godet M, Grosclaude J, Delmas B, Laude H (1994) Major receptor-binding and neutralization determinants are located within the same domain of the transmissible gastroenteritis virus (coronavirus) spike protein. J Virol 68:8008–8016

Greenough TC, Babcock GJ, Roberts A, Hernandez HJ, Thomas WD Jr, Coccia JA, Graziano RF, Srinivasan M, Lowy I, Finberg RW (2005) Development and characterization of a severe acute respiratory syndrome-associated coronavirus-neutralizing human monoclonal antibody that provides effective immunoprophylaxis in mice. J Infect Dis 191:507–514

Hamming I, Timens W, Bulthuis ML, Lely AT, Navis G, van Goor H (2004) Tissue distribution of ACE2 protein, the functional receptor for SARS coronavirus. A first step in understanding SARS pathogenesis. J Pathol 203:631–637

He Y, Zhou Y, Liu S, Kou Z, Li W, Farzan M, Jiang S (2004a) Receptor binding domain of SARS-CoV spike protein induces highly potent neutralizing antibodies: implication for developing subunit vaccine. Biochem Biophys Res Commun 324:773–781

He Y, Zhou Y, Wu H, Luo B, Chen J, Li W, Jiang S (2004b) Identification of immunodominant sites on the spike protein of severe acute respiratory syndrome (SARS) coronavirus: implication for developing SARS diagnostics and vaccines. J Immunol 173:4050–4057

He Y, Zhu Q, Liu S, Zhou Y, Yang B, Li J, Jiang S (2005) Identification of a critical neutralization determinant of severe acute respiratory syndrome (SARS)-associated coronavirus: importance for designing SARS vaccines. Virology 334:74–82

Hofmann H, Hattermann K, Marzi A, Gramberg T, Geier M, Krumbiegel M, Kuate S, Uberla K, Niedrig M, Pöhlmann S (2004) S protein of severe acute respiratory syndrome-associated coronavirus mediates entry into hepatoma cell lines and is targeted by neutralizing antibodies in infected patients. J Virol 78:6134–6142

Hwang WC, Lin Y, Santelli E, Sui J, Jaroszewski L, Stec B, Farzan M, Marasco WA, Liddington RC (2006) Structural basis of neutralization by a human anti-severe acute respiratory syndrome spike protein antibody, 80R. J Biol Chem 281:34610–34616

Imai Y, Kuba K, Rao S, Huan Y, Guo F, Guan B, Yang P, Sarao R, Wada T, Leong-Poi H (2005) Angiotensin-converting enzyme 2 protects from severe acute lung failure. Nature 436:112–116

Komatsu T, Suzuki Y, Imai J, Sugano S, Hida M, Tanigami A, Muroi S, Yamada Y, Hanaoka K (2002) Molecular cloning, mRNA expression and chromosomal localization of mouse angiotensin-converting enzyme-related carboxypeptidase (mACE2). DNA Seq 13:217–220

Kuba K, Imai Y, Rao S, Gao H, Guo F, Guan B, Huan Y, Yang P, Zhang Y, Deng W (2005) A crucial role of angiotensin converting enzyme 2 (ACE2) in SARS coronavirus-induced lung injury. Nat Med 11:875–879

Kuba K, Imai Y, Penninger JM (2013) Multiple functions of angiotensin-converting enzyme 2 and its relevance in cardiovascular diseases. Circ J 77:301–308

Lau SK, Woo PC, Li KS, Huang Y, Tsoi HW, Wong BH, Wong SS, Leung SY, Chan KH, Yuen KY (2005) Severe acute respiratory syndrome coronavirus-like virus in Chinese horseshoe bats. Proc Natl Acad Sci USA 102:14040–14045

Lew RA, Warner FJ, Hanchapola I, Yarski MA, Manohar J, Burrell LM, Smith AI (2008) Angiotensin-converting enzyme 2 catalytic activity in human plasma is masked by an endogenous inhibitor. Exp Physiol 93:685–693

Li W, Moore MJ, Vasilieva N, Sui J, Wong SK, Berne MA, Somasundaran M, Sullivan JL, Luzuriaga K, Greenough TC (2003) Angiotensin-converting enzyme 2 is a functional receptor for the SARS coronavirus. Nature 426:450–454

Li F, Li W, Farzan M, Harrison SC (2005a) Structure of SARS coronavirus spike receptor-binding domain complexed with receptor. Science 309:1864–1868

Li W, Shi Z, Yu M, Ren W, Smith C, Epstein JH, Wang H, Crameri G, Hu Z, Zhang H (2005b) Bats are the natural reservoirs of SARS-like coronaviruses. Science 310:676–679

Oudit GY, Crackower MA, Backx PH, Penninger JM (2003) The role of ACE2 in cardiovascular physiology. Trends Cardiovasc Med 13:93–101

Peiris JSM, Yuen KY (2004) Severe acute respiratory syndrome. Nat Med 10:S88–S97

Prabakaran P, Gan J, Feng Y, Zhu Z, Choudhry V, Xiao X, Ji X, Dimitrov DS (2006) Structure of severe acute respiratory syndrome coronavirus receptor-binding domain complexed with neutralizing antibody. J Biol Chem 281:15829–15836

Rota PA, Oberste MS, Monroe SS, Nix WA, Campagnoli R, Icenogle JP, Peñaranda S, Bankamp B, Maher K, Chen MH (2003) Characterization of a novel coronavirus associated with severe acute respiratory syndrome. Science 300:1394–1399

Sui J, Li W, Murakami A, Tamin A, Matthews LJ, Wong SK, Moore MJ, Tallarico AS, Olurinde M, Choe H (2004) Potent neutralization of severe acute respiratory syndrome (SARS) coronavirus by a human mAb to S1 protein that blocks receptor association. Proc Natl Acad Sci USA 101:2536–2541

Tipnis SR, Hooper NM, Hyde R, Karran E, Christie G, Turner AJ (2000) A human homolog of angiotensin-converting enzyme: cloning and functional expression as a captopril-insensitive carboxypeptidase. J Biol Chem 275:33238–33243

Vickers C, Hales P, Kaushik V, Dick L, Gavin J, Tang J, Godbout K, Parsons T, Baronas E, Hsieh F (2002) Hydrolysis of biological peptides by human angiotensin-converting enzyme-related carboxypeptidase. J Biol Chem 277:14838–14843

Wong SK, Li W, Moore MJ, Choe H, Farzan M (2004) A 193-amino acid fragment of the SARS coronavirus S protein efficiently binds angiotensin converting enzyme 2. J Biol Chem 279:3197–3201

Zhong J, Basu R, Guo D, Chow FL, Byrns S, Schuster M, Loibner H, Wang XH, Penninger JM, Kassiri Z (2010) Angiotensin converting enzyme 2 suppresses pathological hypertrophy, myocardial fibrosis and cardiac dysfunction. Circulation 122:717–728

Zhou T, Wang H, Luo D, Rowe T, Wang Z, Hogan RJ, Qiu S, Bunzel RJ, Huang G, Mishra V (2004) An exposed domain in the severe acute respiratory syndrome coronavirus spike protein induces neutralizing antibodies. J Virol 78:7217–7226

Zhu Z, Chakraborti S, He Y, Roberts A, Sheahan T, Xiao X, Hensley LE, Prabakaran P, Rockx B, Sidorov IA (2007) Potent cross-reactive neutralization of SARS coronavirus isolates by human monoclonal antibodies. Proc Natl Acad Sci USA 104:12123–12128